The nature of carrier localisation in polar and nonpolar InGaN/GaN quantum wells

P. Dawson, S. Schulz, R. A. Oliver, M. J. Kappers, and C. J. Humphreys

Citation: Journal of Applied Physics **119**, 181505 (2016); doi: 10.1063/1.4948237

View online: http://dx.doi.org/10.1063/1.4948237

View Table of Contents: http://aip.scitation.org/toc/jap/119/18

Published by the American Institute of Physics

JOURNAL OF APPLIED PHYSICS **119**, 181505 (2016)

The nature of carrier localisation in polar and nonpolar InGaN/GaN quantum wells

P. Dawson,[1,a)] S. Schulz,[2] R. A. Oliver,[3] M. J. Kappers,[3] and C. J. Humphreys[3]
[1]*School of Physics and Astronomy, Photon Science Institute, University of Manchester, Manchester M13 9PL, United Kingdom*
[2]*Photonics Theory Group, Tyndall National Institute, Dyke Parade, Cork, Ireland*
[3]*Department of Material Science and Metallurgy, 27 Charles Babbage Road, University of Cambridge, Cambridge CB3 0FS, United Kingdom*

(Received 29 October 2015; accepted 29 December 2015; published online 5 May 2016)

In this paper, we compare and contrast the experimental data and the theoretical predictions of the low temperature optical properties of polar and nonpolar InGaN/GaN quantum well structures. In both types of structure, the optical properties at low temperatures are governed by the effects of carrier localisation. In polar structures, the effect of the in-built electric field leads to electrons being mainly localised at well width fluctuations, whereas holes are localised at regions within the quantum wells, where the random In distribution leads to local minima in potential energy. This leads to a system of independently localised electrons and holes. In nonpolar quantum wells, the nature of the hole localisation is essentially the same as the polar case but the electrons are now coulombically bound to the holes forming localised excitons. These localisation mechanisms are compatible with the large photoluminescence linewidths of the polar and nonpolar quantum wells as well as the different time scales and form of the radiative recombination decay curves. [http://dx.doi.org/10.1063/1.4948237]

I. INTRODUCTION

Since the ground breaking work performed[1] by Akasaki, Amano, and Nakamura on InGaN/GaN heterostructures, InGaN light emitting diodes (LEDs) have found widespread applications in many areas such as high brightness displays and solid state lighting. At the heart of these devices are polar InGaN/GaN quantum well (QW) structures grown on sapphire substrates that are capable of generating visible light with high internal quantum efficiencies (IQE).[2–4] For example, blue light emitting LEDs have been fabricated that can exhibit IQE values as high as 90% at room temperature.[5] This remarkable success has been achieved despite the fact that the growth of these high efficiency device substructures occurs on a sapphire substrate, where the lattice mismatch with GaN is 16%.[6] Such a large mismatch leads[7–9] to the epitaxy of nitride based layers with dislocation densities of at least $\sim 10^8\,\mathrm{cm}^{-2}$. This in many ways is contrary to the normal approach to the fabrication of high efficiency III-V optoelectronic devices. Usually, the mismatch between the substrate,[10] GaAs or InP, and the epitaxial layers that do not have the same lattice parameter as the substrate is chosen to be so small that the layers are elastically strained. This avoids the production of high densities of defects that can occur as a result of strain relaxation. This is vital for achieving high IQE values, e.g., in GaAs based devices, it is essential[11] to achieve dislocation densities less than $10^3\,\mathrm{cm}^{-2}$ to prevent the significant non-radiative recombination.

This apparent problem with GaN based structures grown on sapphire should in principle be compounded by the long radiative lifetimes in InGaN/GaN QWs. This occurs because of the large spontaneous and piezoelectric polarisations[12–14] that produce electric fields of $\sim 10^6\,\mathrm{V\,cm}^{-1}$ across the QWs. These fields cause separation of the electron and hole wavefunctions that result in not only increases to the radiative recombination lifetimes but also an associated quantum confined Stark effect[12] that moves the peak of the recombination to lower energies. It is difficult to quantify the increase in radiative lifetimes produced by the built-in electric fields because, as will be discussed in detail later, it is impossible to assign a single time constant to the radiative recombination process. Nevertheless, at low temperatures, energy dependent radiative decay times for InGaN/GaN QWs are quoted[15–18] to be ~10 s of nanoseconds compared with exciton decay times in GaAs/AlGaAs QWs ~100 s of picoseconds.[19] It is widely accepted[18,20–24] that the carrier localisation can, to a large extent, overcome non-radiative recombination associated with defects. However, the role of carrier localisation[25,26] in the process responsible for efficiency reduction at high carrier densities, the so-called efficiency droop,[27,28] is still the subject of extensive discussion. Nevertheless, the effects of carrier localisation go beyond the beneficial effect of reducing the causes of defect-related non-radiative recombination. There are clear implications for the basic optical properties including the form of the emission spectra[29] and the radiative decay curves.[18] Thus, the precise nature of carrier localisation is fundamental to many of the operating characteristics of InGaN based LEDs.

At the same time, there are clear indications that the precise nature of the carrier localisation is not common to all forms of InGaN QWs and that different effects can arise, for example, in nonpolar structures for which the strong macroscopic electric fields across the QWs are absent. There is

a)Electronic mail: philip.dawson@manchester.ac.uk

great interest in the properties of nonpolar InGaN QWs for two main reasons. Firstly, the IQEs of polar InGaN QWs designed to emit in the green[30] part of the spectrum are much less than those that emit in the blue.[31] This behaviour is preventing the full exploitation of the nitride materials system for producing high brightness sources in the green part of the visible spectrum. One possible explanation for this behaviour is that green emitters contain significantly larger fractions of In in the QWs than their blue emitting counter parts. This leads to large elastic strains and hence, in polar materials, much greater radiative lifetimes that can, in the presence of non-radiative recombination paths, lead to reduced values of IQE. Thus, nonpolar QW structures in which there is no macroscopic electric field perpendicular to the plane of the QWs should have relatively short radiative lifetime leading to structures that exhibit high IQE in the green part of the spectrum. Secondly, the in-plane anisotropic strain and differences in the hole effective masses along the growth direction can lead to lifting of the valence band degeneracy that enables the emission of strong linearly polarised light from nonpolar InGaN QW structures.[32,33] Clearly, the presence or absence of the macroscopic intrinsic electric field will impact mainly on the radiative recombination rate but there is a stark contrast between not only the time scale of the recombination dynamics[34] but also the more basic radiative recombination processes[35] for nonpolar and polar InGaN QW structures.

In this paper, we will compare and contrast the nature of the localisation mechanisms in polar and nonpolar InGaN QWs and the consequences for their fundamental optical properties. All the samples discussed here were grown by metalorganic chemical vapor deposition (MOCVD), the polar sample was grown on c plane sapphire using a quasi-two temperature growth methodology which we have described in detail elsewhere,[36] and the nonpolar *m*-plane sample was grown on freestanding bulk GaN as described in Ref. 37. Using a CW excitation power density of 6 W/cm^2 from a He/Cd laser, the room temperature IQE was measured using the methodology[36] of comparing the ratio of the integrated photoluminescence (PL) intensity at room temperature and 10 K. The measured ratios were 10% and 20% for the *c*-plane and *m*-plane samples, respectively. It should be noted that for both the samples, these figures are indicative of good quality material for such a low excitation density. However, since the IQE is a function of carrier density[36] and the carrier density depends on the overall recombination rate and thus on the radiative recombination times, which inevitably differ between the polar and nonpolar samples, these values cannot be directly compared.

II. POLAR QUANTUM WELLS

In Figure 1 is shown a typical low temperature photoluminescence (PL) spectrum from an $In_xGa_{1-x}N$/GaN multiple QW sample. In this particular case, the In fraction in the QW is 0.16 and the QW thickness is 2.5 nm. The nature of the recombination processes responsible for the low temperature spectra has been the subject of a great deal of study, with the generally accepted view that the main emission peak

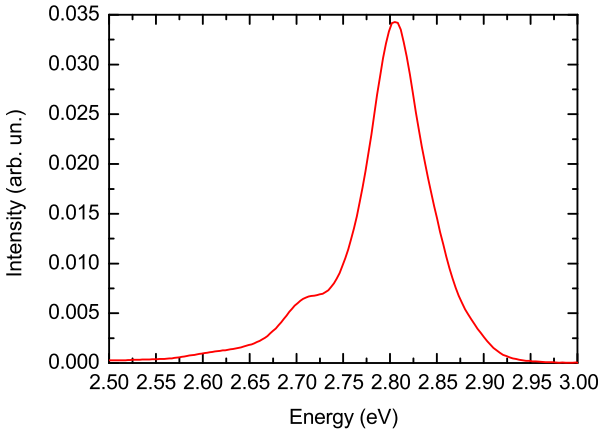

FIG. 1. PL spectrum measured at a temperature of 10 K for polar InGaN/GaN QW structure.

(2.805 eV) involves the recombination of localised carriers with the series of lower energy features that occur with a periodicity ~90 meV being assigned to longitudinal optical (LO) phonon replicas of the main peak.[38] The initial view that the localisation plays a key role was largely based on the linewidth of the zero phonon emission and the temperature dependence of the peak energy. The latter effect was one of the strongest indications of the importance of carrier localisation. The distinctive behaviour of the PL peak energy, which for the spectrum shown in Figure 1 is displayed in Figure 2, is widely referred to as the S shape and has been extensively reported.[39–41] The overall form of the S shape has been explained in terms[40,42] of the thermally driven redistribution of carriers amongst the available localisation sites. It should be stressed that the S shape is fundamentally caused by the changes in the linewidth of the zero phonon line with temperature. Related to the carrier localisation is the form of the PL decay curves at low temperature. In Figure 3 are shown a series of decay curves measured at different detection energies across the spectrum shown in Figure 1. The most important aspects of these curves that relate to the carrier localisation are the non-exponential nature of the decay curves and detection energy dependence

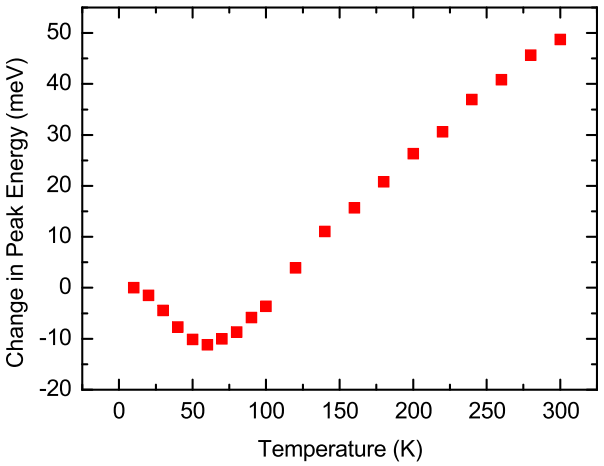

FIG. 2. Change in peak energy of PL spectrum as a function of temperature with the temperature dependence of the InGaN removed from the data.

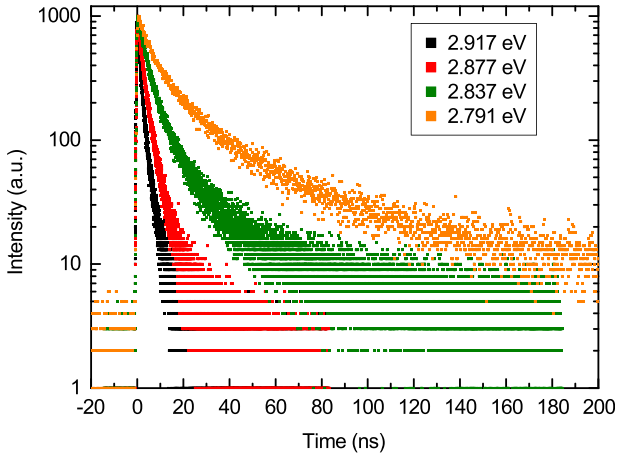

FIG. 3. PL decay curve measures = d at the detection energies indicated for the spectrum shown in Figure 1.

which shows slower decay times with decreasing detection energies across the zero phonon line. Of course, as we discussed earlier the overall time scale of the decays is anticipated to be much longer than in, for example, GaAs QWs. This is due to the spatial separation of the electron hole wavefunctions perpendicular to the plane of the QWs caused by the in-built electric field. As we shall see later, however, this does not explain completely the form of the decay curves and the time scales over which the decays occur.

Despite this powerful evidence for localisation, the precise nature of the localisation has been the subject of extensive debate. A range of localisation mechanisms has been proposed including indium clusters,[20,43–46] QW width fluctuations,[38,47] and random fluctuations in the local In fraction.[48,49] Of these possibilities, the case for In clusters was largely disproved in the work of Smeeton *et al.*[50] and Galtrey *et al.*,[51] who showed that the evidence for In clustering could be attributed to electron beam damage in the TEM measurements.

Nevertheless, the roles of well width fluctuations and random fluctuations in In fraction remain to be considered. This was done independently in the work of Watson-Parris *et al.*[52] and Schulz *et al.*[53] Watson-Parris *et al.* used an effective mass treatment to calculate the potential energies of electrons and holes in an InGaN QW, and specifically how these energies were influenced by the effects of a random distribution of In atoms and well width fluctuations. They found that the holes are strongly localised in regions, where the In fraction is significantly greater than the average and the electrons are less strongly localised by alloy and well width fluctuations, with the electrons in particular, being localised at the top QW interface due to the effects of the in-built electric field. This result was confirmed in a later independent study by Schulz *et al.*[53] using an atomistic tight-binding model. Using this atomistic model, an example of the predicted electron and hole ground states in a 3.5 nm wide $In_{0.25}Ga_{0.75}N$/GaN QW is given in the left hand column of Figure 4 (Single-Particle States). For this work, disk-like well width fluctuations with a diameter of 5 nm and height of 2 monolayers were assumed, which are close to the experimentally reported values.[29] The results shown include

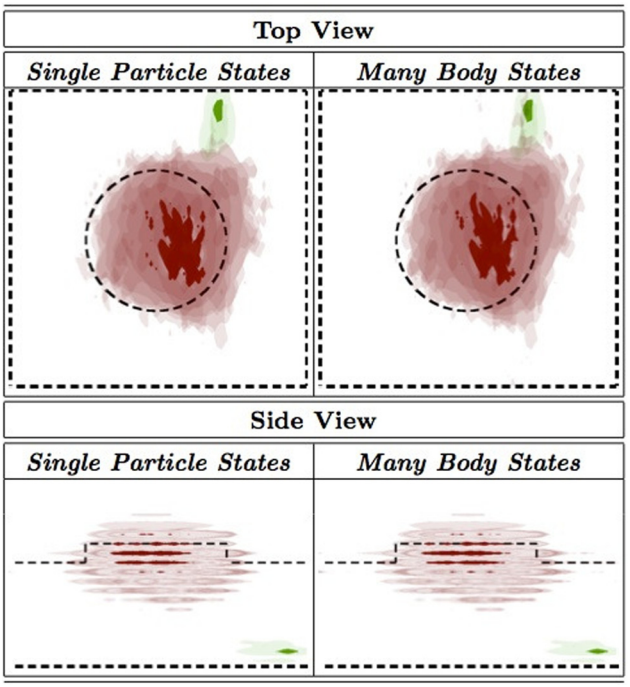

FIG. 4. Isosurfaces of the electron (red) and hole (green) ground state charge densities in an $In_{0.25}Ga_{0.75}N$/GaN QW in the absence (left, Single-Particle States) and in the presence (right, Many-Body States) of Coulomb interaction between the electron and the hole. The light and dark isosurfaces correspond to 5% and 50% of the maximum charge densities. The dashed lines indicate the QW interfaces. The results are shown for a top view (parallel to c-axis) and a side view (perpendicular to the c-axis) of the QW structure. The in-plane super cell dimensions are 10 nm × 9 nm and the QW width is approximately 3.5 nm. The diameter of the disk like well-width fluctuations is 5 nm and the height is 2 monolayers.

random alloy fluctuations and the resulting local variations in strain and built-in potential. Isosurfaces of the electron and hole ground state charge densities are displayed in red and green, respectively. The dashed lines indicate the QW interfaces. Due to the presence of the strong electrostatic built-in field along the growth direction, the electron and hole wave functions are localised at opposite QW interfaces. Figure 4 clearly indicates strong hole wave function localisation effects caused by the random alloy fluctuations. Of particular relevance to the results of the PL spectroscopy mentioned above, Watson-Parris *et al.* and Schulz *et al.* were able to show that the large PL linewidth is due to the fluctuations in the localisation energies of the holes and that the fluctuations in electron localisation are of secondary importance in determining the form of the PL spectrum. This is illustrated in Figure 5 for the electron and hole ground state energies from Schulz's atomistic tight-binding calculations for the InGaN/GaN QW discussed above. Here, for the fixed In content of 25%, the calculations have been repeated 10 times to realise different random atomic configurations in the QW. The results in Figure 5 are depicted as a function of the configuration number n. To visualize the data on the same energy scale, the electron and hole ground state energies are displayed relative to their respective average ground state energies. Figure 5 clearly demonstrates a much larger variation in the hole ground state energies when compared with the electrons. This effect is consistent with the picture

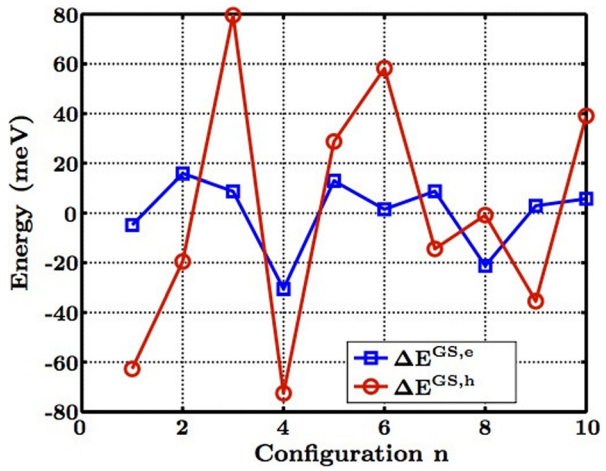

FIG. 5. Relative electron (blue square) and hole (red circle) ground state energies as a function of the microscopic configuration number n. The electron and hole ground state energies are with respect to the ground state energies averaged over the 10 configurations.

of strongly localised hole ground states, which makes these states very sensitive to the local atomic structure and therefore to the microscopic configuration n. So, taking all these factors into account, we are left with a picture of strongly localised holes and electrons that are mainly localised due to the combined effects of the macroscopic built-in electric field, alloy, and well width fluctuations. In this discussion, so far we have ignored any effects of the Coulomb interaction between the electrons and holes and any subsequent excitonic effects. This question was addressed in particular, in the work of Schulz *et al.*,[53] who considered the effects of the Coulomb interaction between the localised electrons and holes. They found that the spatial separation of the electron and hole wavefunctions due to the presence of the built-in potential and the localisation effects is much stronger than the electron/hole Coulomb interaction. An example for this behaviour is shown in the right hand column of Figure 4 (Many-Body States), where excitonic effects are included in the atomistic tight-binding calculations via the configuration interaction scheme. When we compare the electron and hole charge densities in the absence (left) and in the presence (right) of the Coulomb interaction, we find that the charge densities are essentially the same. This indicates that the behaviour of the ground state charge densities is mainly dominated by the localisation effects arising from (i) the macroscopic built-in electric field across the QW, (ii) local alloy fluctuations, and (iii) well width fluctuations. Thus, although the Coulomb interaction introduces a small shift in energy of the predicted low temperature PL spectrum, the electrons and holes can be treated as largely independent. This overall view has very important consequences for the explanation for the recombination dynamics as discussed in detail by Morel *et al.*[54] As shown in Figure 3, at low temperatures, the PL decay curves are non-exponential and vary with detection energy, so that the overall time scale increases with decreasing detection energy across the zero phonon part of the spectrum. Morel *et al.* treated the independently localised electrons and holes as a pseudo two-dimensional donor-acceptor pair system. From this treatment, it was shown that the shape of the decay curves (the non-exponential character) was governed by the statistical distribution of the electron and hole localisation sites in the plane of the QWs. The spectral dependence of the time scale of the decays was explained as being a consequence of the change in strain and hence macroscopic built-in electric field associated with the variations in local In content responsible for the change in hole localisation energy as discussed above. As part of their treatment, Morel *et al.* presented extensive evidence of good agreement between theory and experiment, where the PL intensity decayed by three orders of magnitude.

However, it should be noted that this overall view that at low temperatures, the recombination occurs between independently localised electrons and holes has been questioned in the work of Brosseau *et al.*,[55] who explained the form of the spectrally integrated PL decay curve from one $In_{0.2}Ga_{0.8}N/GaN$ multiple QW sample as being dominated by recombination involving isolated localisation centres.

III. NONPOLAR QUANTUM WELLS

GaN offers two relatively stable growth directions inclined at 90° to the c [0001] direction which are known as a [11$\bar{2}$0] and m [1$\bar{1}$00] that enable the fabrication of nonpolar InGaN/GaN QW structures. Contrary to the case of the growth of polar QW structures, the choice of substrate can strongly influence the nature of the recombination in nonpolar QW structures. For example, if the growth is carried out heteroepitaxially on r-plane sapphire substrates, basal plane stacking faults (BSFs) propagate through the QWs which can lead to an associated recombination path. This problem is eliminated if the QWs are grown on bulk GaN substrates which have no BSFs. Recently, it has been proposed[56] that In clustering occurs in a-plane QWs which could act as localisation centres. Thus, to make the comparison with polar QWs more meaningful, we will concentrate on the carrier localisation mechanisms in m-plane QW structures grown on bulk GaN substrates. The low temperature PL spectrum for a 5 period m-plane InGaN/GaN QW structure whose well width and In fraction were 1.9 nm and 0.17, respectively, is shown in Figure 6. As in the case of spectrum from the polar structure, the FWHM is large at 121 meV, in fact much larger than the width of the spectrum in Figure 1. Previously, we have reported[37] that as the sample was grown on a substrate with a 2° miscut, there are variations in indium content associated with local step features. The greatest variations are associated with large, widely spaced macroscopic steps which give rise to the low energy tail of the spectrum displayed in Figure 6. We were not able to see any evidence for significant inhomogeneity associated with step edges on the main m-plane facets between the step bunches. The contribution to the overall width of the spectrum from the step edge PL is very small and does not influence the quoted value for the FWHM of the spectrum. As we will discuss later, it is not surprising that the spectrum is broad if the effects of random In fluctuations still play a role in determining the recombination mechanism. Extra information can be obtained for nonpolar QWs by measuring the polarised PL

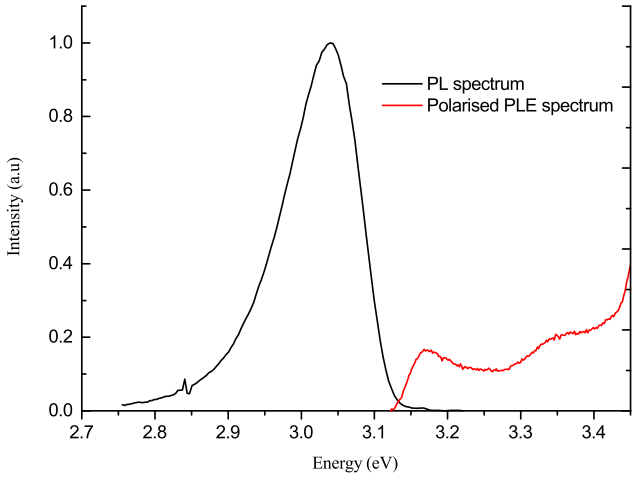

FIG. 6. PL and polarised PLE spectrum for m-plane structure measured at a temperature of 10 K.

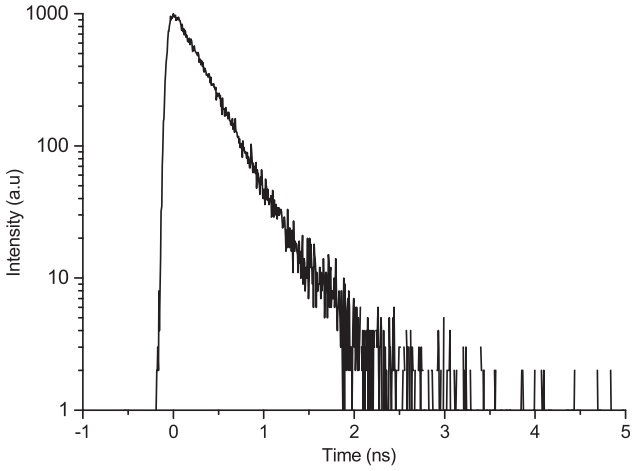

FIG. 7. PL decay curve measured at the peak of the PL spectrum shown in Figure 6 at a temperature of 10 K.

excitation (PLE) spectrum as shown in Figure 6. In this figure, we show only the spectrum in which the excitation light is polarised to the *c* axis of the sample. In this case, we see an exciton transition at 3.171 eV that is associated with the n = 1 electron state and the lowest lying n = 1 strain split valence band.[57] On the assumption that the recombination is intrinsic in nature, then the energy difference between the exciton peak energy in the PLE spectrum and the recombination peak of 131 meV gives us a direct measure of the depth of localisation. As in the case of polar QWs,[52,53] the localisation effects are very large. Although the general form of the PL spectra of nonpolar QWs is not dissimilar from that of polar systems, we note that the one major difference is the absence of any LO phonon assisted recombination. The fundamental cause of the phonon assisted recombination is the separation of the electron and hole wavefunctions not only along the growth direction due to the polarisation induced electric field[29] but also in the plane of the QWs on separate localisation sites.[58] So the absence of the phonon satellites suggests that not only is the polarisation field absent but also the independent localisation of electrons and holes may not occur.

Probably, the biggest contrast in the low temperature optical properties of polar and nonpolar InGaN QWs is in the form and time scale of the radiative recombination dynamics. In Figure 7, we show a typical PL decay curve from an *m*-plane InGaN/GaN multiple QW structure. Clearly, not only is the time scale over which the recombination occurs much shorter than, for example, from a polar system shown in Figure 3 but also is the decay single exponential. This behaviour was first reported by Marcinkevicius *et al.*[35] and put forward in support of the idea that the recombination involves localised excitons.

Support for this concept has recently been put forward by Schulz *et al.*[59] who made a detailed comparison of the theoretical predictions of an atomistic tight binding model with the optical properties of an *m*-plane InGaN/GaN multiple QW structure. They predicted that the fundamental modifications of the properties of nonpolar QWs compared with polar QWs are due to the changes in the nature of the electron localisation due to the absence of the electric field perpendicular to the plane of the QWs. The nature of the hole localisation is largely the same, whereas the absence of the electric field means that the electrons are no longer localised by any well width fluctuations but rather the electron/hole Coulomb interaction is sufficiently strong that the electrons are bound to the holes leading to the localised excitons. An example of the predicted electron and hole ground state charge densities using the model of Schulz *et al.*[59] for a 2 nm wide *m*-plane $In_{0.17}Ga_{0.83}N$/GaN QW is given in Figure 8. The left hand column of Figure 8 shows isosurfaces of the electron (red) and hole (green) ground state charge densities in the absence of the Coulomb interaction (Single Particle States). As described above, the electron charge density is almost spread out over the entire QW region, while the random alloy fluctuations give rise to strong hole wave function localisation. When Coulomb effects are included in the calculations, the charge density of the hole ground state is almost unaffected while the electron localises about the hole.

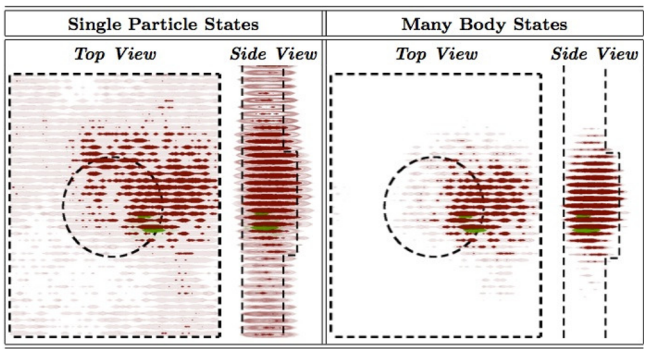

FIG. 8. Isosurfaces of electron (red) and hole (green) ground state charge densities in an m-plane In0.17Ga0.83N/GaN QW. Light and dark isosurfaces correspond to 5% and 25% of the maximum charge density. The results in absence of the Coulomb interaction are displayed on the left hand side (Single Particle States), while the right hand side depicts the data in the presence of the Coulomb interaction (Many Body States). Again the results are shown for different viewpoints: top view (parallel to m-axis) and side view (perpendicular to m-axis). The in-plane super cell dimensions are 10 nm × 9 nm and the QW width is approximately 2 nm. The diameter of the disk like well-width fluctuations is 5 nm and the height is 2 monolayers.

This is illustrated in the right hand column of Figure 8, where the electrons can be seen to be localised to the holes, in contrast to the behaviour shown in the left hand column of Figure 8. Based on this model, Schulz *et al.*[59] obtained very good agreement between the predicted form of the low temperature emission spectrum and a measured spectrum, while the measured single exponential decay curves are also compatible with this picture of localised excitons.

IV. SUMMARY

In summary, we have compared and contrasted the nature of the centres responsible for low temperature carrier localisation in polar and nonpolar InGaN/GaN QWs. Based on independent effective mass and atomistic calculations, it is predicted that in polar systems, the macroscopic built-in electric field localises the electrons at well width fluctuations, whereas the holes are localised at regions of the QWs, where the In fraction is locally high due to the random distribution of In in the InGaN QWs. This model of independently localised electrons and holes is compatible with the measured optical properties. The large low temperature PL linewidth is mainly due to the variations in hole localisation energy, and the energy dependent non-exponential PL decay curves measured at low temperatures is characteristic of independently localised electrons and holes that are separated by varying distances.

Whereas in nonpolar QWs, the fluctuations in the randomly distributed In fraction still localise the holes but because of the absence of the electric field the electrons bind to the holes by coulomb interaction to form localised excitons. Thus, the low temperature PL linewidth is very similar to the case of polar QWs but the form and time scale of the PL decay curves is radically different. Basically, the radiative decay occurs on a much faster time scale compared with the polar QWs but also the decay curves are exponential which reflect the localised exciton character of the emitting centres.

As discussed in Section I, it is widely accepted that at room temperature, carrier localisation plays a significant role in overcoming non-radiative recombination paths associated with the large defect densities in InGaN/GaN QW structures. More precisely, at room temperature where we might expect some degree of in-plane carrier diffusion, it is the characteristic energies of the localisation that will be largely responsible for restricting carrier diffusion. In the case of polar structures, using the independent electron and hole effective mass model described by Watson-Parris *et al.*,[52] it was estimated[26] that for an InGaN QW with an In fraction of 0.12 and an average well width of 3.0 nm, the intrinsic electron diffusion length would be ~250 nm and the intrinsic hole diffusion length would be ~10 nm at room temperature. These figures are compatible with the observation that InGaN/GaN QWs with the dislocation densities as high as $5 \times 10^8\,\mathrm{cm}^{-2}$ can exhibit high photoluminescence IQE at room temperature. This argument can only be regarded as approximate as the density of point defects can also play a role[60] in determining diffusion lengths and hence the IQE. As for nonpolar structures, it can be argued that the carrier localisation may not play as dominant role in determining the room temperature IQE as the radiative lifetime itself is so much shorter than that of polar QWs. Nevertheless, as with polar structures, the carrier localisation plays a major role in determining the form of the spontaneous emission spectrum as well as the recombination mechanism assuming that the localised excitons continue to be the dominant recombination channel at room temperature.

ACKNOWLEDGMENTS

This work was carried out with the support of the United Kingdom Engineering and Physical Sciences Research Council under Grant Nos. EP\J001627\1, EP/I012591/1, EP/H011676/1, and EP\J003603\1, Science Foundation Ireland (SFI) under Project Nos. 13/SIRG/2210 and 10/IN.1/I2994, and the European Union 7th Framework Programme project DEEPEN (Grant Agreement No. 604416). S.S. also acknowledges computing resources at Tyndall provided by SFI and the SFI and Higher Education Authority funded Irish Centre for High End Computing.

We would also like to thank M. J. Godfrey, D. Watson-Parris, T. J. Badcock, D. Sutherland, M. Davies, S. Hammersley, E. P. O'Reilly, M. A. Caro, C. Coughlan, and D. P. Tanner for useful discussions.

[1]See http://www.nobelprize.org/nobel_prizes/physics/laureates/2014/ The Nobel Prize in Physics 2014 was awarded jointly to Isamu Akasaki, Hiroshi Amano and Shuji Nakamura "for the invention of efficient blue light-emitting diodes which has enabled bright and energy-saving white light sources."
[2]Q. Dai, M. F. Schubert, J. K. Kim, D. D. Koleske, M. H. Crawford, S. R. Lee, A. J. Fischer, G. Thaler, and M. A. Banas, Appl. Phys. Lett. **94**, 111109 (2009).
[3]A. Hangleiter, D. Fuhrmann, M. Grewe, F. Hitzel, G. Klewer, S. Lahmann, C. Netzel, N. Riedel, and U. Rossow, Phys. Status Solidi A **201**, 2808 (2004).
[4]Y. L. Li, Y. R. Huang, and Y. H. Lai, Appl. Phys. Lett. **91**, 181113 (2007).
[5]T. Sano, T. Doi, S. A. Inada, T. Sugiyama, Y. Honda, H. Amano, and T. Yoshino, Jpn. J. Appl. Phys., Part 1 **52**, 08JK09 (2013).
[6]S. A. Kukushkin, A. V. Osipov, V. N. Bessolov, B. K. Medvedev, V. K. Nevolin, and K. A. Tcarik, Rev. Adv. Mater. Sci. **17**, 1 (2008).
[7]S. Nakamura, M. Senoh, and T. Mukai, Appl. Phys. Lett. **62**, 2390 (1993).
[8]S. Nakamura, T. Mukai, and M. Senoh, Appl. Phys. Lett. **64**, 1687 (1994).
[9]M. J. Davies, P. Dawson, F. C.-P. Massabuau, F. Oehler, R. A. Oliver, M. J. Kappers, T. J. Badcock, and C. J. Humphreys, Phys. Status Solidi C **11**, 750 (2014).
[10]J. Singh, *Semiconductor Optoelectronics, Physics and Technology* (McGraw-Hill, 1995).
[11]N. Nanhui, W. Huaibing, L. Naixin, H. Yanhui, H. Jun, D. Jun, and J. Guangdi, J. Cryst. Growth **286**, 209 (2006).
[12]T. Takeuchi, S. Sota, M. Katsuragawa, M. Komori, H. Takeuchi, H. Amano, and I. Akasaki, Jpn. J. Appl. Phys., Part 2 **36**, L382 (1997).
[13]F. Bernardini, V. Fiorentini, and D. Vanderbilt, Phys. Rev. B **63**, 193201 (2001).
[14]O. Mayrock, H.-J. Wunsche, and F. Henneberger, Phys. Rev. B **62**, 16870 (2000).
[15]T. Akasaka, H. Gotoh, H. Nakano, and T. Makimoto, Appl. Phys. Lett. **86**, 191902 (2005).
[16]S. F. Chichibu, T. Azuhata, T. Sota, T. Mukai, and S. Nakamura, J. Appl. Phys. **88**, 5153 (2000).
[17]J. Wang, L. Wang, W. Zhao, Z. Hao, and Y. Luo, Appl. Phys. Lett. **97**, 201112 (2010).
[18]J. A. Davidson, P. Dawson, T. Wang, T. Sugahara, J. W. Orton, and S. Sakai, Semicond. Sci. Technol. **15**, 497 (2001).
[19]J. Feldmann, G. Peter, E. O. Gobel, P. Dawson, K. Moore, C. T. Foxon, and R. J. Elliott, Phys. Rev. Lett. **59**, 2337 (1987).

[20]S. Chichibu, K. Wada, and S. Nakamura, Appl. Phys. Lett. **71**, 2346 (1997).
[21]K. L. Teo, J. S. Coulton, P. S. Yu, E. R. Weber, M. F. Li, W. Liu, K. Uchida, H. Tokunaga, N. Akutsa, and K. Matsumoto, Appl. Phys. Lett. **73**, 1697 (1998).
[22]J. Bai, T. Wang, and S. Sakai, J. Appl. Phys. **88**, 4729 (2000).
[23]I. L. Krestnikov, N. N. Ledentsov, A. Hoffman, D. Bimberg, A. V. Sakharov, W. V. Lundin, A. F. Tsatsul'nikov, A. S. Usikov, and D. Gerthsen, Phys. Rev. B **66**, 155310 (2002).
[24]H. Schomig, S. Halm, A. Forchel, G. Bacher, J. Off, and F. Scholz, Phys. Rev. Lett. **92**, 106802 (2004).
[25]J. Hader, J. V. Moloney, and S. W. Koch, Appl. Phys. Lett. **96**, 221106 (2010).
[26]S. Hammersley, D. Watson-Parris, P. Dawson, T. J. Godfrey, M. J. Kappers, C. McAleese, R. A. Oliver, and C. J. Humphreys, J. Appl. Phys. **111**, 083512 (2012).
[27]H. Morkoc, *Handbook of Nitride Semiconductors and Devices* (Wiley VCH, Berlin, 2008), Vol. 3.
[28]J. Xie, X. Ni, Q. Fan, R. Shimada, U. Ozgur, and H. Morkoc, Appl. Phys. Lett. **93**, 121107 (2008).
[29]S. Kalliakos, X. B. Zhang, T. Taliercio, P. Lefebvre, B. Gil, N. Grandjean, B. Damilano, and J. Massies, Appl. Phys. Lett. **80**, 428 (2002).
[30]H. Y. Ryu, G. H. Ryu, S. H. Lee, and H. J. Kim, J. Korean Phys. Soc. **63**, 180 (2013).
[31]M. J. Cich, R. I. Aldaz, A. Chakraborty, A. David, M. J. Grundmann, A. Tyagi, M. Zhang, F. M. Steranka, and M. R. Krames, Appl. Phys. Lett. **101**, 223509 (2012).
[32]T. Guhne, Z. Bougrioua, S. Laught, M. Nemoz, P. Vennegues, B. Vinter, and M. Leroux, Phys. Rev. B **77**, 075308 (2008).
[33]T. Paskova, Phys. Status Solidi B **245**, 1011 (2008).
[34]G. A. Garrett, H. Shen, M. Wraback, A. Tyagi, M. C. Schmidt, J. S. Speck, S. P. DenBaars, and S. Nakamura, Phys. Status Solidi C **6**, S800 (2009).
[35]S. Marcinkevicius, K. M. Kelchner, L. Y. Kuritzky, S. Nakamura, S. P. DenBaars, and J. S. Speck, Appl. Phys. Lett. **103**, 111107 (2013).
[36]R. A. Oliver, F. C.-P. Massbuau, M. J. Kappers, W. A. Phillips, E. J. Thrush, C. C. Tartan, W. E. Blenkhorn, T. J. Badcock, P. Dawson, M. A. Hopkins, D. W. Allsopp, and C. J. Humphreys, Appl. Phys. Lett. **103**, 141114 (2013).
[37]D. Sutherland, T. Zhu, J. T. Griffiths, F. Tang, P. Dawson, D. Kundys, F. Oehler, M. J. Kappers, C. J. Humphreys, and R. A. Oliver, Phys. Status Solidi B **252**, 965 (2015).
[38]D. M. Graham, A. Soltani-Vala, P. Dawson, M. J. Godfrey, T. M. Smeeton, J. S. Barnard, M. J. Kappers, C. J. Humphreys, and E. J. Thrush, J. Appl. Phys. **97**, 103508 (2005).
[39]P. G. Eliseev, P. Perlin, J. Lee, and M. Osinski, Appl. Phys. Lett. **71**, 569 (1997).
[40]P. G. Eliseev, M. Osinski, J. Lee, T. Sugahara, and S. Sakai, J. Electron. Mater. **29**, 332 (2000).
[41]Y. H. Cho, G. H. Gainer, A. J. Fischer, J. J. Song, S. Keller, U. K. Mishra, and S. P. DenBaars, Appl. Phys. Lett. **73**, 1370 (1998).
[42]O. Rubel, S. D. Baranovskii, J. D. Hantke, J. Koch, P. Thomas, J. M. Marshalla, W. Stolz, and W. W. Ruhle, J. Optoelectron. Adv. Mater. **7**, 115 (2005).
[43]Y. Narukawa, Y. Kawakami, M. Funato, M. Fujita, S. Fujita, and S. Nakamura, Appl. Phys. Lett. **70**, 981 (1997).
[44]Y. Narukawa, Y. Kawakami, S. Fujita, and S. Nakamura, Phys. Rev. B **55**, R1938 (1997).
[45]K. P. O'Donnell, R. W. Martin, and P. G. Middleton, Phys. Rev. Lett. **82**, 237 (1999).
[46]P. Ruterana, S. Kret, A. Vivet, G. Maciejewski, and P. Dluzewski, J. Appl. Phys. **91**, 8979 (2002).
[47]J. Narayan, H. Wang, J. Ye, S.-J. Hon, K. Fox, J. C. Chen, H. K. Choi, and J. C. Fan, Appl. Phys. Lett. **81**, 841 (2002).
[48]L. Bellaiche, T. Mattila, L.-W. Wang, S.-H. Wei, and A. Zunger, Appl. Phys. Lett. **74**, 1842 (1999).
[49]L.-W. Wang, Phys. Rev. B **63**, 245107 (2001).
[50]T. M. Smeeton, M. J. Kappers, J. S. Barnard, M. E. Vickers, and C. J. Humphreys, Appl. Phys. Lett. **83**, 5419 (2003).
[51]M. J. Galtrey, R. A. Oliver, M. J. Kappers, C. J. Humphreys, P. Clifton, D. Larson, D. Saxey, and A. Cerezo, J. Appl. Phys. **104**, 013524 (2008).
[52]D. Watson-Parris, M. J. Godfrey, P. Dawson, R. A. Oliver, M. J. Galtrey, M. J. Kappers, and C. J. Humphreys, Phys. Rev. B **83**, 115321 (2011).
[53]S. Schulz, M. A. Caro, C. Coughlan, and E. P. O'Reilly, Phys. Rev. B **91**, 035439 (2015).
[54]A. Morel, P. Lefebvre, S. Kalliakos, T. Taliercio, T. Bretagnon, and B. Gil, Phys. Rev. B **68**, 045331 (2003).
[55]C.-N. Brosseau, M. Perrin, C. Silva, and R. Leonelli, Phys. Rev. B **82**, 085305 (2010).
[56]F. Tang, T. Thu, F. Oehler, W. Y. Fen, J. T. Griffiths, F. C.-P. Massabuau, M. J. Kappers, T. J. Martin, P. A. Bagot, M. P. Moody, and R. A. Oliver, Appl. Phys. Lett. **106**, 072104 (2015).
[57]T. J. Badcock, P. Dawson, M. J. Kappers, C. McAleese, J. L. Hollander, C. F. Johnston, D. V. Sridhara Rao, A. M. Sanchez, and C. J. Humphreys, J. Appl. Phys. **105**, 123112 (2009).
[58]S. Kalliakos, X. B. Zhang, T. Talierco, P. Lefebvre, B. Gil, N. Grandjean, B. Damilano, and J. Massies, Appl. Phys. Lett. **80**, 428 (2002).
[59]S. Schulz, D. P. Tanner, E. P. O'Reilly, M. A. Caro, D. Sutherland, M. J. Davies, P. Dawson, F. Tang, J. T. Griffiths, F. Oehler, M. J. Kappers, R. A. Oliver, and C. J. Humphreys, Phys. Rev. B **92**, 235419 (2015).
[60]S. Hammersley, M. J. Kappers, F. C.-P. Massabuau, S.-L. Sahonta, P. Dawson, R. A. Oliver, and C. J. Humphreys, Appl. Phys. Lett. **107**, 132106 (2015).